

University of Nebraska - Lincoln
DigitalCommons@University of Nebraska - Lincoln

Faculty Publications from The Water Center

Water Center, The

3-15-2014

Improving the treatment of non-aqueous phase TCE in low permeability zones with permanganate

Chanat Chokeyaroenrat

Suranaree University of Technology, chanat@sut.ac.th

Steve D. Comfort

University of Nebraska-Lincoln, scomfort1@unl.edu


Chainarong Sakulthaew

Kasetsart University, cvtcns@ku.ac.th

Bruce I. Dvoark

University of Nebraska-Lincoln, bdvorak1@unl.edu

Follow this and additional works at: <http://digitalcommons.unl.edu/watercenterpubs>

 Part of the [Hydraulic Engineering Commons](#), [Hydrology Commons](#), and the [Other Environmental Sciences Commons](#)

Chokeyaroenrat, Chanat; Comfort, Steve D.; Sakulthaew, Chainarong; and Dvoark, Bruce I., "Improving the treatment of non-aqueous phase TCE in low permeability zones with permanganate" (2014). *Faculty Publications from The Water Center*. 27.
<http://digitalcommons.unl.edu/watercenterpubs/27>

This Article is brought to you for free and open access by the Water Center, The at DigitalCommons@University of Nebraska - Lincoln. It has been accepted for inclusion in Faculty Publications from The Water Center by an authorized administrator of DigitalCommons@University of Nebraska - Lincoln.

Improving the treatment of non-aqueous phase TCE in low permeability zones with permanganate

Chanat Chokejaroenrat,^{1, 2} Steve Comfort,³ Chainarong Sakulthaew,^{3, 4} and Bruce Dvorak¹

1. Department of Civil Engineering, University of Nebraska–Lincoln, Lincoln, NE 68588-0531, USA; bdvorak1@unl.edu
2. School of Environmental Engineering, Institute of Engineering, Suranaree University of Technology, Nakhon Ratchasima 30000, Thailand; chanat@sut.ac.th
3. School of Natural Resources, University of Nebraska–Lincoln, Lincoln, NE 68583-0915, USA
4. Department of Veterinary Technology, Kasetsart University, Bangkok 10900, Thailand; cvtcns@ku.ac.th

Corresponding author — S. Comfort, tel 402 472-1502, fax 402 472-7904, email scomfort1@unl.edu

Abstract

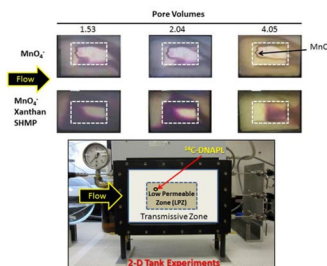
Treating dense non-aqueous phase liquids (DNAPLs) embedded in low permeability zones (LPZs) is a particularly challenging issue for injection-based remedial treatments. Our objective was to improve the sweeping efficiency of permanganate (MnO_4^-) into LPZs to treat high concentrations of TCE. This was accomplished by conducting transport experiments that quantified the penetration of various permanganate flooding solutions into a LPZ that was spiked with non-aqueous phase ^{14}C -TCE. The treatments we evaluated included permanganate paired with: (i) a shear-thinning polymer (xanthan); (ii) stabilization aids that minimized MnO_2 rind formation and (iii) a phase-transfer catalyst. In addition, we quantified the ability of these flooding solutions to improve TCE destruction under batch conditions by developing miniature LPZ cylinders that were spiked with ^{14}C -TCE. Transport experiments showed that MnO_4^- alone was inefficient in penetrating the LPZ and reacting with non-aqueous phase TCE, due to a distinct and large MnO_2 rind that inhibited the TCE from further oxidant contact. By including xanthan with MnO_4^- , the sweeping efficiency increased (90%) but rind formation was still evident. By including the stabilization aid, sodium hexametaphosphate (SHMP) with xanthan, permanganate penetrated 100% of the LPZ, no rind was observed, and the percentage of TCE oxidized increased. Batch experiments using LPZ cylinders allowed longer contact times between the flooding solutions and the DNAPL and results showed that SHMP + MnO_4^- improved TCE destruction by ~16% over MnO_4^- alone (56.5% vs. 40.1%). These results support combining permanganate with SHMP or SHMP and xanthan as a means of treating high concentrations of TCE in low permeable zones.

Keywords: xanthan, permanganate, TCE, stabilization aids, In situ chemical oxidation

Highlights

- Transport experiments used transmissive and low permeability zones (LPZs).
- ^{14}C -labeled TCE was used to quantify oxidation of DNAPL in LPZs by permanganate.
- Stabilization aids prevented MnO_2 rind formation.
- DNAPL oxidation improved when xanthan and stabilization aids were used.

Graphical abstract



1. Introduction

The release of dense non-aqueous liquids (DNAPL) into the subsurface typically results in the formation of disconnected blobs

and ganglia depending on the soil's physical heterogeneity [1, 2]. Dissolved contaminants migrating from DNAPL source zones will often diffuse from transmissive regions into low permeable zones (LPZs). The residual build up of contaminants in LPZs over time

becomes particularly challenging for injection-based remedial treatments because chemical oxidants typically bypass low porosity zones. Given that the mass of contaminant stored in low permeability soils can be substantial and that these LPZs can serve as a long-term source of contamination, removing chlorinated solvents like trichloroethene (TCE) from low permeability zones is recognized as one of the most difficult problems associated with groundwater pollution [3].

Although permanganate is extremely efficient in oxidizing TCE [4, 5], treating non-aqueous phase TCE trapped in low permeable zones has significant challenges. When permanganate (MnO_4^-) is used, the three hurdles to successfully treating non-aqueous phase TCE in LPZs include: (i) getting the MnO_4^- to penetrate and not bypass lower porosity zones where the contaminant is located, (ii) minimizing MnO_2 rind formation at the MnO_4^- -DNAPL interface, which can block or inhibit the DNAPL from further oxidant contact, and (iii) overcoming the kinetic constraints of treating a sparingly soluble DNAPL with an aqueous-phase oxidant. While significant progress has been made in combating these challenges, improving the treatment of chlorinated solvents in LPZs is still an active area of research.

To get remedial fluids to penetrate LPZs, shear-thinning polymers like xanthan have been used as a co-injected remedial agent to increase the viscosity of the displacing fluid [6–13] and stimulate cross-flow between layers that differ in permeability [14, 15]. Smith et al. [16] provided the first evidence that xanthan was compatible with MnO_4^- and could be used as a polymer-enhanced chemical oxidation treatment for perchloroethylene (PCE). Their work provided important groundwork for further studies aimed at determining what polymer and oxidant concentrations were needed to effectively oxidize chlorinated solvents in low permeability zones during transport. McCray et al. [17] showed that use of xanthan increased the sweeping efficiency of MnO_4^- into LPZs (containing non-aqueous phase PCE) and improved the percentage PCE oxidized. Recently, Chokejaroenrat [18] found that adding xanthan enhanced MnO_4^- delivery into LPZs to treat aqueous-phase TCE and minimized the potential for rebound.

Treating non-aqueous phase TCE with MnO_4^- is more challenging than treating aqueous phase TCE due to the higher propensity for manganese dioxide (MnO_2) to form. Many researchers who have treated non-aqueous phase DNAPL with MnO_4^- have reported the formation of distinct MnO_2 rinds, which can protect the contaminant from further contact with the oxidant e.g., [19–24]. Moreover, substantial MnO_2 deposits have the potential to alter the advective flow of the oxidant from the target zone [23, 25–27]. One way researchers have combated this problem is by recognizing that soluble Mn(IV) and colloidal Mn(IV) precede the aggregation and formation of the insoluble MnO_2 product. This has given rise to the use of stabilization aids. Mata-Perez and Perez-Benito [28] found that the conversion rate of soluble Mn(IV) to MnO_2 (s) could be delayed when phosphate was present. Kao et al. [29] found that ~82% of MnO_2 production could be inhibited by including Na_2HPO_4 with MnO_4^- without affecting TCE loss. Crimi and Ko [30] tested a variety of stabilization aids and reported that sodium hexametaphosphate (SHMP) was superior in minimizing MnO_2 formation.

Phase transfer catalysts are agents that facilitate reactions between two or more phases (i.e., polar, non-polar) and allow reactions to occur that otherwise might be inhibited [31]. The idea for using phase-transfer catalysts would be to allow some of the oxidant (i.e., MnO_4^-) to partition into the non-aqueous phase DNAPL so that oxidation can occur in both the organic and bulk aqueous phases and reduce the time needed to remove the non-aqueous phase product. Seol and Schwartz [32] and Seol et al. [33] used the phase transfer catalyst, pentyltriphenylphosphonium bromide

(PTPP) in bench studies and reported increased dechlorination of both TCE and PCE. Although the initial results were promising, reports of using phase-transfer catalysts under transport conditions have not yet been reported.

In this study, our objective was to improve the sweeping efficiency of MnO_4^- into LPZ and increase the percentage of ^{14}C -TCE oxidized by MnO_4^- . This was accomplished by creating a LPZ that had a high concentration of TCE and then treating with a variety of solutions that paired permanganate with: (i) a shear-thinning polymer; (ii) stabilization aids that minimized MnO_2 formation and (iii) a phase-transfer catalyst. Both transport and batch experiments were performed to quantify the efficacy of these chemical additives to improve TCE oxidation.

2. Materials and methods

2.1. Chemicals and soils

Trichloroethene (TCE; C_2HCl_3 ; ACS reagent, $\geq 99.5\%$), Oil-Red-O (an organic-soluble dye, $\text{C}_{26}\text{H}_{24}\text{N}_4\text{O}$), hydrazine hydrate (35 wt% in H_2O), xanthan gum (CAS-11138-66-2) and ethyl acetate were obtained from Sigma-Aldrich (St. Louis, MO). Potassium permanganate (KMnO_4) was obtained from Fisher Scientific (Pittsburgh, PA). Additional chemicals included: acetonitrile (Midland Scientific), nitric acid (J.T. Baker, Phillipsburgh, NJ), and sodium hydroxide (Fisher Scientific, Pittsburgh, PA).

Stabilization aids included sodium hexametaphosphate (SHMP, Sigma Aldrich) and tetrapotassium pyrophosphate (TKPP; Carus Corporation). Uniformly labeled ^{14}C -TCE (specific activity of 5 mCi mmol $^{-1}$) was obtained from Moravek Biochemicals (Brea, CA). The phase transfer catalyst evaluated was pentyltriphenylphosphonium bromide (PTPP; Sigma Aldrich). A listing of physiochemical properties of the chemicals used is provided in Supplementary material (SM) section (Table SM-1).

Soils used in transport experiments were chosen to create a transmissive zone and a low permeability zone (LPZ). The transmissive zone was packed with commercial silica sand (Accusand 20/30, Le Sueur, MN) while the low permeable zone was fabricated by mixing a silty clay loam with a silica sand (Accusand 40/50) in a 1:16 (w/w) ratio. The silty clay loam was used to increase mass of TCE retained by the LPZ [34]. This silty clay loam was obtained from a loess deposit ~6.1 m below ground surface on the University of Nebraska campus (Lincoln, NE).

Details on procedures used to analyze TCE, MnO_4^- and ^{14}C -activity are provided in the SM section.

2.2. Transport experiments

2.2.1. 2D-tank

All transport experiments were conducted in the specifically designed rectangular anodized aluminum tank (2D-Tank) consisting of three chambers. The main chamber (1061 cm 3) housed the soil and had internal dimensions of 21.6 cm (length) by 12.7 cm (height) by 5.1 cm (width) (Figure 1). The 2D-tank was hand packed with a rigorous set of steps and procedures to ensure uniformity between experiments. Details of these packing procedures are provided in the SM section.

The 2D-tank was initially dry-packed by hand to yield a calculated bulk density of 1.76 kg m $^{-3}$ for the transmissive zone and 1.57 kg m $^{-3}$ for the LPZ zone. The packed systems had an approximate average porosity of 0.38 and a total pore volume (PV) of ~481 cm 3 .

Prior to flooding, we exchanged the air space in the 2D-tank with carbon dioxide gas (CO_2) for 60 min. This prevented entrapped air pockets from forming in the tank during flooding [35].

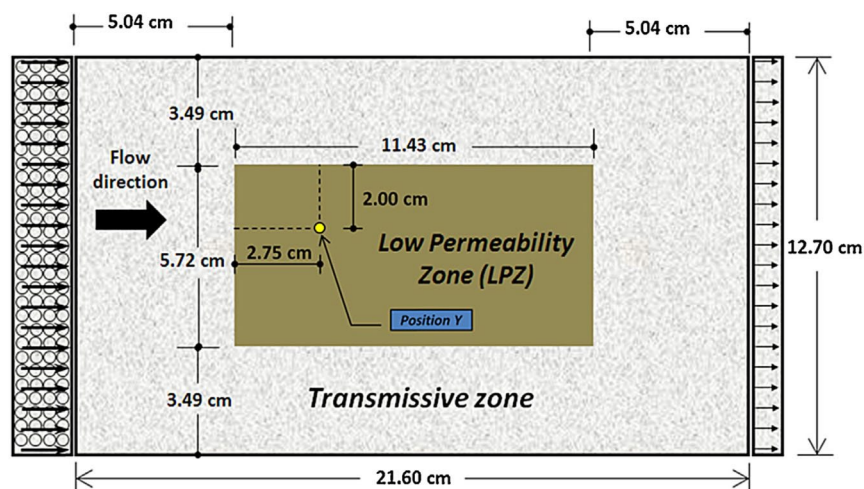


Figure 1. Size and dimensions of transmissive and low permeable zones used in 2D-tank experiments. Non-aqueous phase ^{14}C -TCE was placed at position “Y”.

We initially flooded the system with background electrolyte concentration ($441 \text{ mg L}^{-1} \text{ CaCl}_2 \cdot 2\text{H}_2\text{O}$). Once flooded, the system was rested for 24 h prior to adding non-aqueous phase TCE to the LPZ.

2.2.2. Adding non-aqueous phase TCE to the low permeable zone

To make it easier to view, TCE was dyed with Oil-Red-O (Table SM-1) at a concentration of 40.8 mg L^{-1} . Previous results have shown that adding this dye did not significantly affect the viscosity, interfacial tension, and density of PCE [36]. Non-aqueous phase TCE (2.0 mL) was spiked with ^{14}C -TCE to produce an initial activity of $\sim 350,000 \text{ dpm}$. This ^{14}C -spiked non-aqueous phase TCE was then introduced directly into the porous media from the top of the tank by using a 5-mL glass syringe equipped with a 22G needle (Hamilton Company, Reno, NV) (Figure 1; Position Y). During the injection, we simultaneously withdrew solution from the LPZ using another glass syringe to balance pressure in the tank and to avoid overflow. We then reassembled the tank and allowed 24 h of resting prior to commencing the experiments.

Given that high entry pressures normally inhibit free phase DNAPL from penetrating low permeability zones, we acknowledge that injecting 2 mL of DNAPL into the LPZ deviates from what might normally occur under field conditions (i.e., temporal build up of dissolved contaminants in LPZs through diffusion). Still, given that DNAPL distribution is typically characterized by highly irregular patterns of residual droplets or ganglia, the probability of some DNAPL droplets surrounded by lower conductivity media exist. Moreover, fissures, cracks or larger pores could also bring DNAPL into a low conductivity zones, as could “organic wetting” constituents (indigenous to the aquifer or built up with time), which have been shown to facilitate the penetration of DNAPL into lower permeability layers [37].

2.2.3. General flooding procedure

A flooding solution was prepared 2 h prior to starting experiments. We used a MnO_4^- concentration of 9931 mg L^{-1} in our transport experiments (Exp. A-F; Table SM-2). In experiments involving chemical additives (Exp. B–F), the chemical amendments (i.e., xanthan, SHMP, TKPP, or PTPP) were completely dissolved in H_2O before KMnO_4 was added. To prepare the xanthan stock solution, we slowly added xanthan powder to H_2O while stirring to avoid powder formation of the glass wall. Because xanthan preparation can directly affect the solution viscosity [38], once mixed, the xanthan stock solution (2 g L^{-1}) was continuously mixed on a magnetic stirrer for 90 min at room temperature (25°C) and used within 2 h. Using xanthan within this timeframe avoided any sig-

nificant changes in viscosity [18].

Each sequential transport experiment received approximately 16 pore volume (PV) of flooding solution in two stages: (1) an initial KMnO_4 flood with or without chemical additives (0.5 PV), and (2) a secondary flood of $441 \text{ mg L}^{-1} \text{ CaCl}_2 \cdot 2\text{H}_2\text{O}$ ($\sim 15.5 \text{ PV}$) (Table SM-2). Initial and secondary flooding solutions were introduced into the 2D-tank at a consistent flow rate at 3 mL min^{-1} using HPLC pump (Shimadzu Scientific Instruments, Columbia, MD). A constant flow rate through the tank was confirmed by manually measuring the outflow from the effluent ports. A digital camera (Canon 870 IS) was used to record solute movement and coverage of the LPZ. Sweeping efficiency [9, 17, 39] was qualitatively determined by the percentage of LPZ that was visibly covered by the flooding solution and recorded as a function of pore volumes (PV) of flooding solution injected. At the end of each experiment, the tank was disassembled and soil selectively removed to visually observe and photograph the LPZ.

2.2.4. Sample collection protocol

Effluent exiting the 2D-tank was quantitatively collected in 1-L collapsible Tedlar bags equipped with a stainless steel valves (Zefon, Ogala, FL) [40]. To minimize volatilization, any gas produced from the MnO_4^- -TCE reaction (i.e., CO_2), was frequently removed using an air-tight glass syringe. We initially added 1 mL hydrazine solution (35 wt% in H_2O) to the Tedlar bags to quench the MnO_4^- [4]. The bag was agitated by hand every 30 min so that the freshly collected effluent was always in contact with hydrazine and the MnO_4^- quenched.

Samples were periodically collected from the Tedlar bags after approximately 420 mL of effluent had been collected (i.e., 0.85 PV; 140 min). At each sampling, three 8-mL samples were withdrawn from the bag by using a 10-mL glass syringe with a luer-lock connector. We then used the procedures outlined in Kriegman-King and Reinhard [41] to differentiate between $^{14}\text{CO}_2$, non-volatile degradation products, and parent TCE.

2.3. Testing the ability of permanganate with and without chemical amendments to oxidize non-aqueous phase TCE under batch conditions

To allow longer contact between the chemical treatments (MnO_4^- + amendments) and non-aqueous phase TCE, as opposed to the timeframe exhibited during the transport experiments, batch experiments were conducted in a 40-mL Teflon tubes. Two types of batch experiments were conducted. In the first set, 100 μL

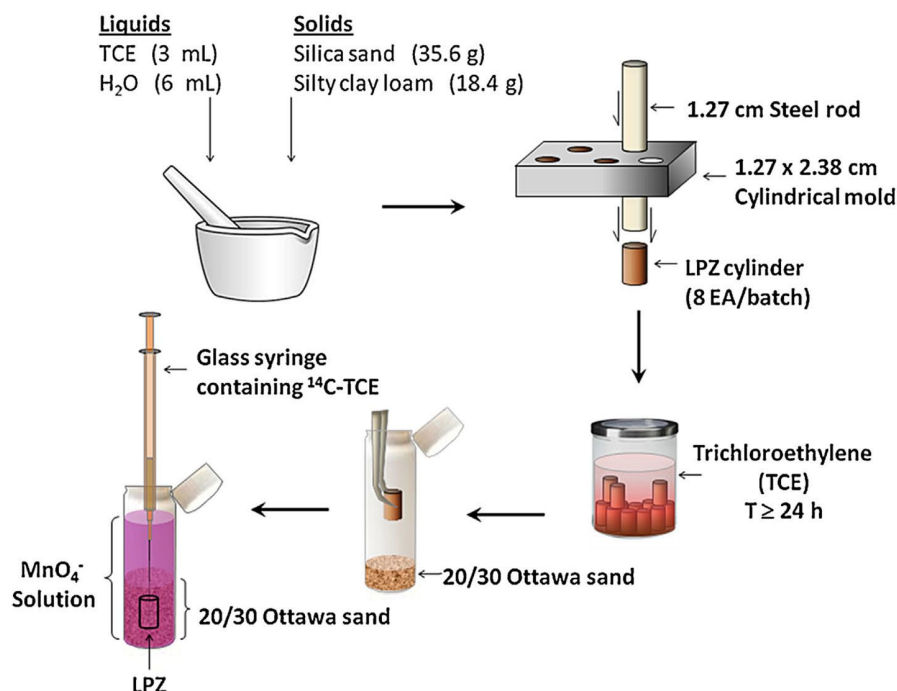


Figure 2. Process used to create low-permeable zone (LPZ) cylinders for batch experiments.

of non-aqueous phase TCE was initially placed in the bottom of the tube containing 13.5 g of silica sand (Accusand 20/30). Additional experimental details of this experiment and results are presented in the SM section.

For the second set of batch experiments, cylinders of low permeable soil containing non-aqueous phase ^{14}C -TCE were created. These LPZ soil cylinders were created by combining two soil textures. Specifically, 35.6 g of silica sand (Accusand 40/50) was combined with 18.4 g of silty clay loam (the same soil used in the transport experiments) and blended manually in a porcelain mortar (Figure 2, SM-1). We then mixed in 3 mL of non-aqueous phase TCE (i.e., DNAPL) and 6 mL of H_2O to increase the liquid content and produce a soil mixture that was pliable and had consistent shear strength. We then packed 6 g of this soil mixture into the cylindrical molds (1.27 cm diam \times 2.38 cm length). These LPZ cylinders were then removed from the mold and soaked in non-aqueous phase TCE for at least 24 h in an effort to saturate the system (see Figure SM-1 for photograph). Each LPZ soil cylinder weighed 6.0 ± 0.1 g before saturating and 6.3 ± 0.1 g after saturating. Given that DNAPL volume and its interfacial area can directly affect mass transfer [42], the weight and surface area of the LPZ cylinders were reproduced to be as consistent as possible.

After soaking in TCE, LPZ cylinders were placed on top of 8.5 g of 20/30 sand in 40-mL vials. We then quickly surrounded the LPZ cylinder with 26.5 g of 20/30 sand and 10 mL of treatment solution. We then introduced 25 μL of ^{14}C -TCE directly into LPZ via a 50- μL glass syringe (Hamilton Company, Reno, NV) (Figure 2). The total activity added to each LPZ cylinder was 22,200 dpm, which was confirmed via liquid scintillation counting (LSC). We then filled the vessel with the rest of the treatment solution leaving no head space. Each vial was weighed before and after introducing any sand and chemicals to determine the precise volume of solution in each replicate. Once the solution treatments were added, the vials were sealed with Teflon-lined septa with open-top screw caps.

The experimental treatments tested six different solution treatments ($n = 3$). These included: (1) control (no MnO_4^-); (2) MnO_4^- ; (3) $\text{MnO}_4^- + \text{PTPP}$; (4) $\text{MnO}_4^- + \text{SHMP}$; (5) $\text{MnO}_4^- + \text{TKPP}$; and (6) $\text{MnO}_4^- + \text{xanthan} + \text{SHMP}$. Concentration of chemical addi-

tives were the same as those used in the transport experiments (Table SM-2). Each group was also subcategorized into two MnO_4^- concentrations (i.e., 12,000, and 24,000 mg L^{-1}).

Each experimental treatment ($n = 3$) was analyzed once the MnO_4^- was consumed ($T = 14$ d). For each experimental unit, we split the analysis into determining the activity of the top solution (Portion 1) and the extracted activity of the sand and LPZ cylinder (Portion 2). Collectively, the ^{14}C -activity of Portions 1 and 2 constituted the activity for each sample. Details on how recovery of ^{14}C -TCE was calculated are provided in the SM section.

3. Results

3.1. Transport experiments

Multiple transport experiments were performed and photographed to systematically evaluate the ability of MnO_4^- to penetrate the LPZ and react with the non-aqueous phase TCE, with and without chemical additives (Figure 3). Using only MnO_4^- , the injection front moved quickly through the transmissive zone and eventually into the LPZ (Figure 3, Exp. A). Within 1.5 PV, a distinct rind of precipitated MnO_2 began to form around the non-aqueous phase TCE. Eventually, the rind engulfed much of the LPZ and red-dyed TCE was still evident inside the LPZ (Figure 3). As a result, much of the LPZ was untouched by the MnO_4^- , and the sweeping efficiency of the LPZ only reached 60% (Figure 4).

When xanthan was part of the MnO_4^- flooding solution, more complete penetration of MnO_4^- into the LPZ occurred earlier and the sweeping efficiency increased to 90% by 2 PV (Figure 4). Previous publications have reported similar benefits of using shear-thinning polymers to increase fluid penetration into LPZs [6–9, 18]. Although xanthan improved the sweeping efficiency, multiple MnO_2 rinds still developed (Figure 3). In related work where aqueous-phase TCE (500 mg L^{-1}) occupied the LPZ instead of non-aqueous phase TCE, rind formation was not observed [18].

When the stabilization aid SHMP was included with xanthan and MnO_4^- , the sweeping efficiency increased to 100% (Figure 4)

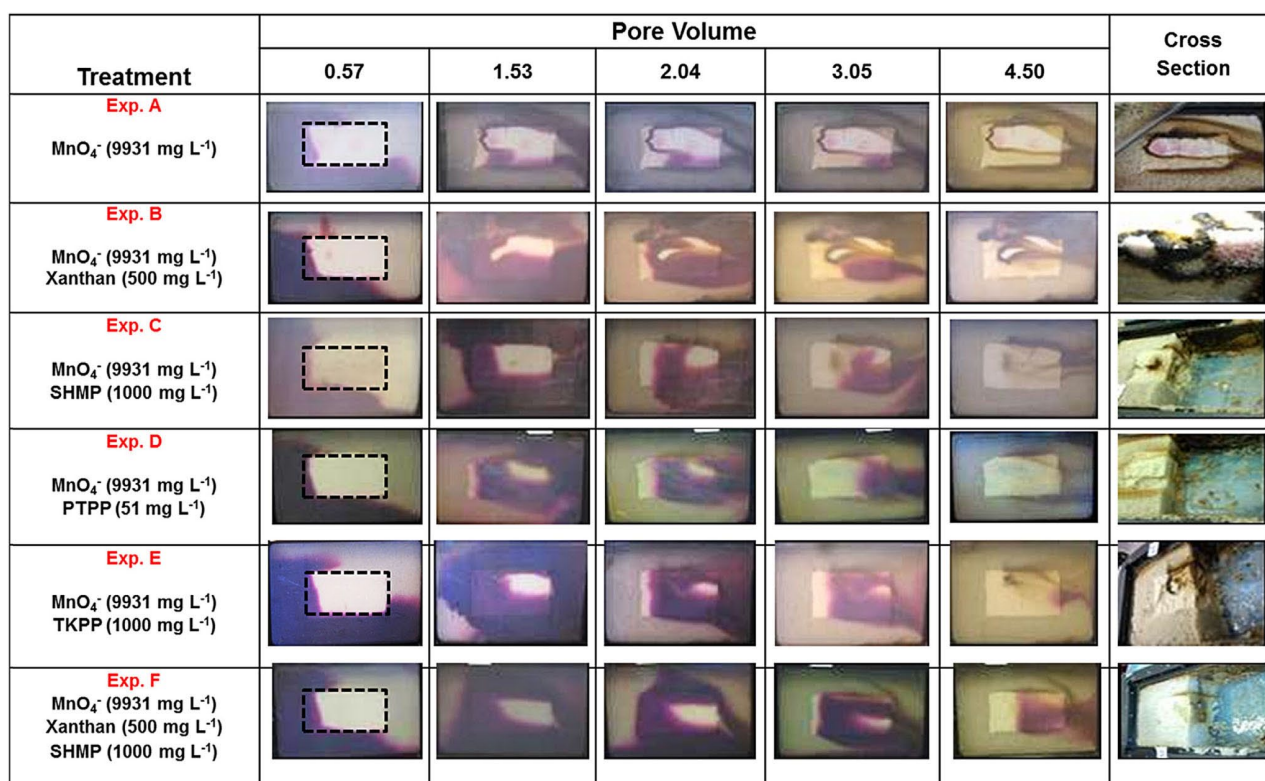


Figure 3. Photographs of 2D-tank following initial and secondary flooding treatments (Exps. A–F).

and no rind was observed (Figure 3, Exp. F). It is noteworthy that while adding SHMP improved the “xanthan + MnO₄⁻” treatment by minimizing MnO₂ formation, similar improvements in permanganate sweeping efficiencies were also observed by including

just the stabilization aids. For instance, when the stabilization aids SHMP and TKPP were paired with MnO₄⁻, we also observed good penetration of MnO₄⁻ into the LPZ with no obvious rind formation (Figure 3). The lack of rind formation similarly produced high sweeping efficiencies (Figure 4).

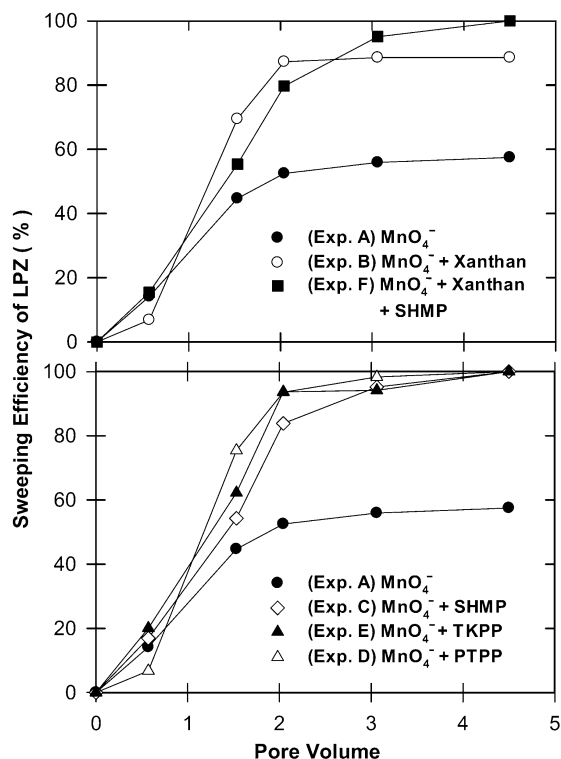


Figure 4. Percent sweeping efficiency of flooding treatments to cover LPZ.

3.1.1. Delineating ¹⁴C-effluent

Delineating the 2D-tank effluent into oxidized ¹⁴C-TCE versus non-oxidized ¹⁴C-TCE, and total ¹⁴C revealed as expected, that less ¹⁴C-activity was recovered from the MnO₄⁻ only treatment due to the MnO₂ rind that formed around the TCE (Exp. A, Figure 5). Although xanthan increased the sweeping efficiency of MnO₄⁻ into the LPZ (Exp. B, Figure 4), the rinds that formed around the non-aqueous product prevented the MnO₄⁻ from interacting with the TCE. This resulted in very little difference between the MnO₄⁻ only and MnO₄⁻ + xanthan treatments in terms of the amount of TCE that was oxidized (11% vs. 13%) or eluted from the 2D-tank (Figure 5). However, by including SHMP with the xanthan, the percentage of oxidized TCE products increased to 19% (8% more than MnO₄⁻ alone) and about 30% more total ¹⁴C was eluted from the tank (Figure 5, SHMP + xanthan + MnO₄⁻ vs. xanthan + MnO₄⁻).

When the three chemical additives (SHMP, TKPP, PTPP) were used individually with MnO₄⁻, there was a 4% to 6% increase in the cumulative amount of oxidized products eluted over MnO₄⁻ alone (Oxidized ¹⁴C-TCE, Figure 5). Because all three chemical additives similarly improved the sweeping efficiency of MnO₄⁻ into the LPZ and prevented a rind from forming around the non-aqueous phase TCE, the percentage of cumulative ¹⁴C-TCE and Total ¹⁴C eluted were greater with the chemical additives than with MnO₄⁻ alone (Figure 5). Although treatment differences between SHMP, TKPP, PTPP were small, the order in which the chemicals increased the ¹⁴C eluted was consistent: SHMP > PTPP > TKPP (Figure 5).

Although the “MnO₄⁻ + SHMP + xanthan” treatment performed the best in terms of the mass of TCE oxidized and total ¹⁴C eluted, pairing SHMP or PTPP with permanganate performed almost as well (Figure 5). Although effective, one argument against

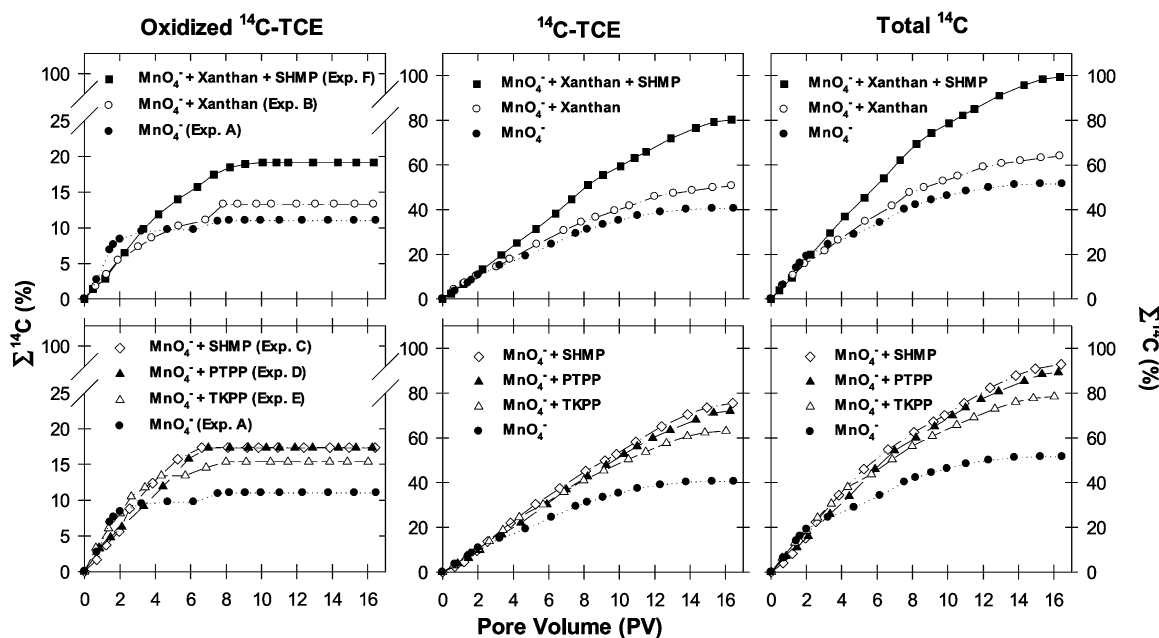


Figure 5. Cumulative ^{14}C eluted (Oxidized, CE and Total) from 2D-tank following initial and secondary flooding treatments (Exps. A–F).

using xanthan is its lack of temporal stability in the presence of permanganate. Previous work by Chokejaroenrat et al. [18] recommended that permanganate–xanthan combinations be used within a few hours of mixing.

3.2. Batch experiments

3.2.1. TCE in sand

Because practically all of the interactions between MnO_4^- and TCE occur at the non-aqueous phase TCE–water boundary and the length of the 2D-tank is finite, the potential to quantify how the chemical additives improved TCE destruction under miscible displacement is limited. To provide supporting evidence, we treated non-aqueous phase TCE with MnO_4^- and the individual chemical additives under batch conditions and monitored temporal changes in TCE recovered (Figure SM-2) and MnO_4^- concentrations (Figure SM-3). In these static reactors, TCE recovered after 14 d showed that SHMP resulted in more TCE loss than PTPP or TKPP. This was especially evident at the 8000 mg L^{-1} MnO_4^- concentration where SHMP resulted in 19% more loss of TCE than MnO_4^- alone and ~8% more than other two chemicals (i.e., PTPP and TKPP, Figure SM-2). A parallel experiment tracked temporal changes in solution pH for the various flooding treatments and the mass of filterable MnO_2 produced. Results showed that SHMP and TKPP produced the least amount of filterable MnO_2 while flooding solutions containing xanthan produced the most (Table SM-3).

3.2.2. TCE in LPZ cylinders

To provide supporting evidence to the results garnered from the 2D-tank (Section 3.1) and batch experiments (Section 3.2.1), our objective was to quantify the efficacy of chemical additives to increase the oxidation of non-aqueous phase TCE by MnO_4^- in low permeable zones under batch conditions. To accomplish this we created a batch reactor that contained a LPZ (containing non-aqueous phase TCE) surrounded by transmissive sands (Figure 2). A test of this experimental unit showed that when the non-aqueous phase ^{14}C -TCE was placed in the LPZ cylinder, the LPZ was effective in holding the ^{14}C -TCE and did not release significant amounts of ^{14}C -TCE back into solution (Figure SM-4). By compar-

ison non-aqueous phase TCE placed in sand (controls) was subject to loss (Figure SM-4). This means treatment solutions needed to penetrate the LPZ cylinders in order to be effective in coming in contact with the ^{14}C -TCE.

By mimicking the treatments used in the transport (Figure 3) and first batch experiment (Figure SM-2), we found that SHMP, TKPP, and PTPP all increased the amount of TCE that was oxidized in the LPZ cylinders. At the $24,000 \text{ mg L}^{-1}$ MnO_4^- concentration, the mass of ^{14}C -TCE recovered was 16% less with SHMP than with MnO_4^- alone; TKPP and PTPP also performed similarly (Figure 6). Given that the ^{14}C -TCE was located inside the LPZ cylinder and not readily released as displayed in our previous test of the LPZ cylinder (Figure SM-4), the results from this experiment indicate that all three chemical amendments facilitated the treatment of TCE while inside a low permeable zone under static conditions.

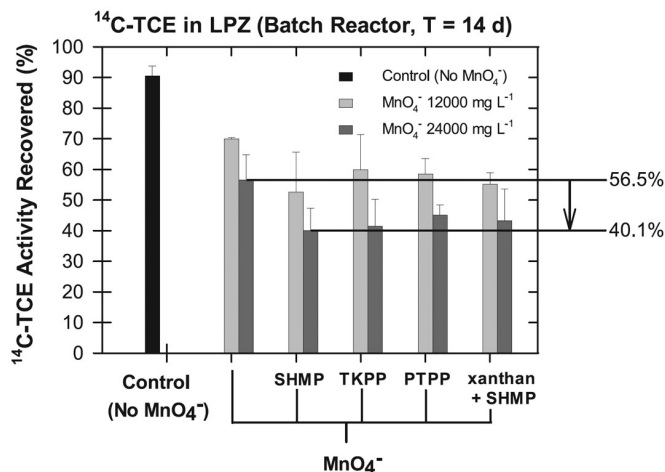


Figure 6. Percent ^{14}C (oxidized, TCE, and total) from batch experiment following with MnO_4^- treatment at 14 d with and without chemical additives (i.e., PTPP, SHMP, TKPP). Each experimental unit contained a LPZ cylinder spiked with ^{14}C -TCE. Bars on symbols represent sample standard deviation of means ($n = 3$).

4. Discussion

SHMP and TKPP are considered dispersants or stabilization aids, which mean they stabilize colloids by inhibiting particle aggregation, which leads to precipitation. The multiple mechanisms by which this occurs with MnO_4^- have been detailed elsewhere [30, 43–46] but in brief the colloidal stability of hydrous oxides is strongly dependent on their net charge. The higher the net charge of the oxide surface, either positive or negative, the greater the repulsive forces of the individual colloid to oppose other colloids and inhibit aggregation (i.e., greater stability). Given that manganese oxides are amphoteric, the net surface charge of the oxide can be altered to negative, zero, or positive. Under most environmental conditions (i.e., pH), manganese dioxide (δMnO_2) is an important adsorbent of phosphate in natural waters [47] and SHMP and TKPP are polyphosphates that can supply soluble phosphate ions. This phosphate can then bind with colloidal oxides, alter the surface charge (i.e., stabilize) and slow the particle coagulation process.

PTPP on the other hand is a phosphorus-centered organic cation (for structure, see Figure SM-5) that has been used as a phase transfer catalyst to increase oxidant concentrations in nonpolar organic phases. Since initially proposed [48], phase transfer catalysts have become a powerful tool in developing new types of reactions in organic chemistry [32]. The use of phase-transfer catalyst in an environmental context has only been sparingly studied. Seol and Schwartz [32] and Seol et al. [33] found that PTPP paired with MnO_4^- increased the dechlorination rate of TCE and PCE. Experiments by Seol and Schwartz [32] were confined to 60 min batch reactions where Cl^- released and MnO_4^- consumed were measured and used to corroborate an improved rate of TCE removal. In our experiments, we directly measured temporal losses of TCE and MnO_4^- for 120 h under static conditions and 8 h under agitated conditions. While results showed a very slight and consistent increase in TCE loss with PTPP among the experiments and concentrations tested (Figure SM-6), these small differences, coupled with the relatively high cost of PTPP, does not appear to warrant supporting its use as a phase-transfer catalyst with MnO_4^- .

Although PTPP did not significantly improve the destruction of non-aqueous phase TCE in a water matrix (Figure SM-6), PTPP did improve the loss of non-aqueous phase TCE by MnO_4^- in the batch experiments (Figs. SM-3, 6). We also observed a high sweeping efficiency when PTPP was included with MnO_4^- under transport conditions (Figure 4), and minimal MnO_2 formation in the LPZ (Figure 3). The results from these various experiments indicate that the ability of PTPP to improve non-aqueous phase TCE destruction do not appear tied to its phase-transfer capabilities but rather to its ability to minimize MnO_2 formation. Unlike SHMP and TKPP, which loads colloids with phosphate ions, sorption of PTPP itself (organic cation) by the colloids may have minimized MnO_2 in the LPZ. Supporting evidence for this mechanism is provided by Posselt et al. [49] who added a nitrogen-based organic cation (polydiallyldimethyl ammonium, PDADMA) to a colloid hydrous manganese dioxide solution and was able to increase the positive charge of the colloids and improve colloidal stabilization (i.e., prevent precipitation). Similar results with clay colloids and PDADMA was observed by Black et al. [50]. Despite its effectiveness as a stabilization aid with permanganate, the high cost of PTPP (in comparison to SHMP and TKPP) would likely preclude its use in the field.

Although we recognized that the xanthan amendment could not provide shear thinning properties under static (i.e., no flow) conditions, we included it in our batch experiments for completeness. Results showed that the xanthan + SHMP + MnO_4^- treatment was similar to the SHMP + MnO_4^- treatment (Figure 6). While adding xanthan with permanganate can cause some MnO_2 formation, the presence of xanthan does not appear to

hinder the beneficial effects of adding SHMP with MnO_4^- , even if this treatment solution were to become trapped in a static zone of an aquifer.

5. Conclusion

Improvements in the treatment of high concentrations of TCE in low permeability zones were accomplished by pairing permanganate with xanthan and stabilization aids. Using xanthan with MnO_4^- improved the sweeping efficiency of permanganate into LPZs but MnO_2 rinds prevented good contact between the oxidant and the DNAPL. By including sodium hexametaphosphate (SHMP) with xanthan, MnO_4^- covered all of LPZ and no MnO_2 rinds were observed. Batch experiments with LPZ cylinders also demonstrated that SHMP improved permanganate oxidation of TCE. While a number of site conditions and cost factors must first be considered before using xanthan and SHMP under field conditions, our experimental results support combining permanganate with SHMP, or SHMP and xanthan, as a means of increasing the mass of TCE oxidized in low permeability zones.

References

- [1] J.W. Mercer, R.M. Cohen, A review of immiscible fluids in the subsurface: properties, models, characterization and remediation, *J. Contam. Hydrol.* 6 (1990) 107–163.
- [2] T.H. Illangasekare, J.L. Ramsey, K.H. Jensen, M.B. Butts, Experimental-study of movement and distribution of dense organic contaminants in heterogeneous aquifers, *J. Contam. Hydrol.* 20 (1995) 1–25.
- [3] H.F. Stroo, M. Unger, C.H. Ward, M.C. Kavanaugh, C. Vogel, A. Leeson, J.A. Marqusee, B.P. Smith, Remediating chlorinated solvent source zones, *Environ. Sci. Technol.* 37 (2003) 224A–230A.
- [4] Y.E. Yan, F.W. Schwartz, Oxidative degradation and kinetics of chlorinated ethylenes by potassium permanganate, *J. Contam. Hydrol.* 37 (1999) 343–365.
- [5] X.D. Li, F.W. Schwartz, DNAPL remediation with in situ chemical oxidation using potassium permanganate. Part I. Mineralogy of Mn oxide and its dissolution in organic acids, *J. Contam. Hydrol.* 68 (2004) 39–53.
- [6] K.E. Martel, R. Martel, R. Lefebvre, P.J. Gelinat, Laboratory study of polymer solutions used for mobility control during in situ NAPL recovery, *Ground Water Monit. Rem.* 18 (1998) 103–113.
- [7] R. Martel, A. Hebert, R. Lefebvre, P. Gelinat, U. Gabriel, Displacement and sweep efficiencies in a DNAPL recovery test using micellar and polymer solutions injected in a five-spot pattern, *J. Contam. Hydrol.* 75 (2004) 1–29.
- [8] T. Robert, R. Martel, S.H. Conrad, R. Lefebvre, U. Gabriel, Visualization of TCE recovery mechanisms using surfactant-polymer solutions in a two-dimensional heterogeneous sand model, *J. Contam. Hydrol.* 86 (2006) 3–31.
- [9] L. Zhong, M. Oostrom, T.W. Wietsma, M.A. Covert, Enhanced remedial amendment delivery through fluid viscosity modifications: Experiments and numerical simulations, *J. Contam. Hydrol.* 101 (2008) 29–41.
- [10] L. Zhong, J. Szecsody, M. Oostrom, M. Truex, X. Shen, X. Li, Enhanced remedial amendment delivery to subsurface using shear thinning fluid and aqueous foam, *J. Hazard. Mater.* 191 (2011) 249–257.
- [11] L. Zhong, M. Oostrom, M.J. Truex, V.R. Vermeul, J.E. Szecsody, Rheological behavior of xanthan gum solution related to shear thinning fluid delivery for subsurface remediation, *J. Hazard. Mater.* 244–245 (2013) 160–170.
- [12] J.A.K. Silva, M. Liberatore, J.E. McCray, Characterization of bulk fluid and transport properties for simulating polymer-improved aquifer remediation, *J. Environ. Eng.* 14 (2013) 9–15, 9.
- [13] J.A.K. Silva, M.M. Smith, J. Munakata-Marr, J.E. McCray, The effect of system variables on in situ sweep-efficiency improvements via viscosity modification, *J. Contam. Hydrol.* 136 (2012) 117–130.

- [14] S.K. Bajjal, *Flow Behavior of Polymers in Porous Media*, Pennwell Publishing Company, Tulsa, OK, 1982.
- [15] L.W. Lake, *Enhanced Oil Recovery*, Prentice-Hall Inc., Englewood Cliffs, NJ, 1989.
- [16] M.M. Smith, J.A.K. Silva, J. Munakata-Marr, J.E. McCray, Compatibility of polymers and chemical oxidants for enhanced groundwater remediation, *Environ. Sci. Technol.* 42 (2008) 9296–9301.
- [17] J.E. McCray, J. Munakata-Marr, J.A.K. Silva, S. Davenport, M.M. Smith, Multiscale experiments to evaluate mobility control methods for enhancing the sweep efficiency of injected subsurface, in: SERDP Project No. ER-1486, 2010.
- [18] C. Chokejaroenrat, N. Kananizadeh, C. Sakulthaew, S.D. Comfort, Y. Li, Improving the sweeping efficiency of permanganate into low permeable zones to treat TCE: Experimental results and model development, *Environ. Sci. Technol.* 47 (2013) 13031–13038.
- [19] X.D. Li, F.W. Schwartz, Efficiency related to permanganate oxidation schemes, in: G.B. Wickramanayake, A.R. Gavaskar, A.S.C. Chen, eds., *Chemical Oxidation and Reactive Barriers: Remediation of Chlorinated and Recalcitrant Compounds*, Battelle Press, Columbus, OH, 2000, pp. 41–48.
- [20] X.D. Li, F.W. Schwartz, DNAPL remediation with in situ chemical oxidation using potassium permanganate. Part II. Increasing removal efficiency by dissolving Mn oxide precipitates, *J. Contam. Hydrol.* 68 (2004) 269–287.
- [21] L.K. MacKinnon, N.R. Thomson, Laboratory-scale in situ chemical oxidation of perchloroethylene pool using permanganate, *J. Contam. Hydrol.* 56 (2002) 49–74.
- [22] M.A. Urynowicz, R.L. Siegrist, Interphase mass transfer during chemical oxidation of TCE DNAPL in aqueous system, *J. Contam. Hydrol.* 80 (2005) 93–106.
- [23] J.L. Heiderscheidt, R.L. Siegrist, T.H. Illangasekare, Intermediate-scale 2-D experimental investigation of in situ chemical oxidation using potassium permanganate for remediation of complex DNAPL source zones, *J. Contam. Hydrol.* 102 (2008) 3–16.
- [24] J.C. Marble, K.C. Carroll, H. Janousek, M.L. Brusseau, In situ oxidation and associated mass-flux-reduction/mass-removal behavior for systems with organic liquid located in lower-permeability sediments, *J. Contam. Hydrol.* 117 (2010) 82–93.
- [25] M. Schroth, M. Oostrom, T.W. Wietsma, J.D. Istok, In-situ oxidation of trichloroethene by permanganate: Effects on porous medium hydraulic properties, *J. Contam. Hydrol.* 29 (2001) 205–224.
- [26] S.H. Conrad, R.J. Glass, W.J. Peplinski, Bench-scale visualization of DNAPL remediation processes in analog heterogeneous aquifers: Surfactant floods and in situ oxidation using permanganate, *J. Contam. Hydrol.* 58 (2002) 13–49.
- [27] X.D. Li, F.W. Schwartz, DNAPL mass transfer and permeability reduction during in situ chemical oxidation with permanganate, *Geophys. Res. Lett.* 31 (2004) L06504.
- [28] F. Mata-Perez, J.F. Perez-Benito, Identification of the product from the reduction of permanganate ion by trimethylamine in aqueous phosphate buffers, *Can. J. Chem.* 63 (1985) 988–992.
- [29] C.M. Kao, K.D. Huang, J.Y. Wang, T.Y. Chen, H.Y. Chien, Application of potassium permanganate as an oxidant for in situ oxidation of trichloroethylenecontaminated groundwater: A laboratory and kinetics study, *J. Hazard. Mater.* 153 (2008) 919–927.
- [30] M. Crimi, S. Ko, Control of manganese dioxide particles resulting from in situ chemical oxidation using permanganate, *Chemosphere* 74 (2009) 847–853.
- [31] B.G. Petri, N.R. Thomson, M.A. Urynowicz, Fundamentals of ISCO using Permanganate, in: R.L. Siegrist, M.C. Thomas, J. Simpkin, eds., *In Situ Chemical Oxidation for Groundwater, SERDP and ESTCP Remediation Technology Monograph Series*, Springer, New York, NY, 2011.
- [32] Y. Seol, F.W. Schwartz, Phase-transfer catalysis applied to the oxidation of nonaqueous phase trichloroethylene by potassium permanganate, *J. Contam. Hydrol.* 44 (2000) 185–201.
- [33] Y. Seol, F.W. Schwartz, S. Lee, Oxidation of binary dnapl mixtures using potassium permanganate with a phase transfer catalyst, *Ground Water Monit. Rem.* 21 (2001) 124–132.
- [34] T.C. Sale, J.A. Zimbron, D.S. Dandy, Effects of reduced contaminant loading on downgradient water quality in an idealized two-layer granular porous media, *J. Contam. Hydrol.* 102 (2008) 72–85.
- [35] W. Littmann, *Polymer Flooding*, Elsevier Science Publishers, New York, NY, 1988.
- [36] K.D. Pennell, G.A. Pope, L.M. Abriola, Influence of viscous and buoyancy forces on the mobilization of residual tetrachloroethylene during surfactant flushing, *Environ. Sci. Technol.* 30 (1996) 1328–1335.
- [37] D.M. O'Carroll, S.A. Bradford, L.M. Abriola, Infiltration of PCE in a system containing spatial wettability variations, *J. Contam. Hydrol.* 73 (2004) 39–63.
- [38] C.S.H. Chen, E.W. Sheppard, Conformation and hydrolytic stability of polysaccharide from *Xanthomonas-campestris*, *J. Macromol. Sci., Chem.* 13 (1979) 239–259.
- [39] J.D. Neil, H.L. Chang, T.M. Geffen, Waterflooding and improved waterflooding, in: F.H. Poettmann, D.C. Bond, C.R. Hocott, eds., *Improved Oil Recovery*, Interstate Oil Compact Commission, Oklahoma City, OK, 1983, p. 363.
- [40] K.C. Huang, G.E. Hoag, P. Chheda, B.A. Woody, G.M. Dobbs, Chemical oxidation of trichloroethylene with potassium permanganate in a porous medium, *Adv. Environ. Res.* 7 (2002) 217–229.
- [41] M.R. Kriegman-King, M. Reinhard, Transformation of carbon tetrachloride in the presence of sulfide, biotite, and vermiculite, *Environ. Sci. Technol.* 26 (1992) 2198–2206.
- [42] K. Kim, M.D. Gurol, Reaction of nonaqueous phase TCE with permanganate, *Environ. Sci. Technol.* 39 (2005) 9303–9308.
- [43] E. Hewitson, N.Y. Rochester, Method of preventing precipitation of alkaline-earth metal salts in gelatin. U.S. Patent 2,256,390, 1941.
- [44] F. Freeman, J.C. Kappos, Permanganate ion oxidations. 15. Additional evidence for formation of soluble (colloidal) manganese dioxide during the permanganate ion oxidation of carbon-carbon double bonds in phosphate-buffered solutions, *J. Am. Chem. Soc.* 107 (1985) 6628–6633.
- [45] M. Crimi, M. Quickel, S. Ko, Enhanced permanganate in situ chemical oxidation through MnO₂ particle stabilization: Evaluation in 1-D transport systems, *J. Contam. Hydrol.* 105 (2009) 69–79.
- [46] R.G. Ball, *Soil and Water Remediation Method and Apparatus: US 2010/0150657*, United States Patent Application Publication, 2010.
- [47] W. Yao, F.J. Millero, Adsorption of phosphate on manganese dioxide in seawater, *Environ. Sci. Technol.* 30 (1996) 536–541.
- [48] C.M. Starks, Phase-transfer catalysis. I. Heterogeneous reactions involving anion transfer by quaternary ammonium and phosphonium salts, *J. Am. Chem. Soc.* 93 (1971) 195–199.
- [49] H.S. Posselt, A.H. Reidies, W.J. Weber Jr., Coagulation of colloidal hydrous manganese dioxide, *J. Am. Water Works Assoc.* 60 (1968) 48–68.
- [50] A.P. Black, F.B. Birkner, J.J. Morgan, Destabilization of dilute clay suspensions with labeled polymers, *J. Am. Water Works Assoc.* 57 (1965) 1547–1560.

Appendix A. Supplementary data follows.

Supporting Material (SM) for:

Improving the treatment of non-aqueous phase TCE in low permeable zones with permanganate

Chanat Chokejaroenrat^{a,b}, Steve Comfort^{c,*}, Chainarong Sakulthaew^{c,d}, and Bruce Dvorak^a

^a *Department of Civil Engineering, University of Nebraska, Lincoln, NE 68583-0531, USA*

^b *School of Environmental Engineering, Institute of Engineering, Suranaree University of Technology, Nakorn Ratchasima, Thailand 30000,*

^c *School of Natural Resources, University of Nebraska, Lincoln, NE 68583-0915, USA*

^d *Department of Veterinary Technology, Kasetsart University, Bangkok, 10900, Thailand*

* Corresponding author Tel.: +001 1 402 4721502; fax: +001 1 402 4727904.

E-mail addresses: chanat@sut.ac.th (C. Chokejaroenrat), scomfort1@unl.edu (S.D. Comfort), cvtcns@ku.ac.th (C. Sakulthaew), bdvorak1@unl.edu (B,I, Dvorak)

Contents

Materials and methods

Chemical analyses

2D-Tank packing procedure

Procedures used to extract and analyze LPZs cylinders

Results and discussion

Tables

Table SM-1 Chemical properties

Table SM-2 Solutions, concentrations, and pore volumes used in transport experiments

Table SM-3 Temporal changes in pH of flooding solutions used to treat non-aqueous phase TCE under batch conditions.

Figures

Figure SM-1 Photographs of low-permeable zone (LPZ) cylinders used in batch experiments

Figure SM-2 Effect of MnO_4^- , with and without chemical amendments, on non-aqueous phase TCE recovery. TCE was placed in transmissive sands in a batch reactor.

Figure SM-3 Temporal changes in MnO_4^- concentrations following treatment of non-aqueous phase TCE with various MnO_4^- flooding solutions. TCE was placed in transmissive sands in a batch reactor.

Figure SM-4 Release of ^{14}C -TCE into solution from non-aqueous TCE that was placed in batch reactor containing sand versus a LPZ cylinder.

Figure SM-5 Pentyltriphenylphosphonium Bromide (PTPP) molecular structure.

Figure SM-6 Tests of the phase-transfer catalyst, PTPP, on improving TCE removal by MnO_4^- under static and agitated conditions.

Acknowledgments

Funding was provided in part by the EPA Region 7, Project ER-0635. Partial support was also provided by the University of Nebraska-Lincoln School of Natural Resources and Water Sciences Laboratory. This paper is a contribution of Agricultural Research Division Projects NEB-38-071.

Materials and methods

Chemical analyses

Temporal changes in TCE concentrations were analyzed by High-Performance Liquid Chromatography (HPLC) equipped with a photodiode array detector (Shimadzu Scientific Instruments, Columbia, MD). Peak separations were achieved by injecting 5 μL of sample into a C-18, 250 x 4.6 mm column, (Supelco, Sigma-Aldrich Corporation, PA) coupled with a guard column (Thermo Scientific, MA). The mobile phase was an isocratic mixture of acetonitrile and H_2O (80:20) at a flow rate of 1.00 mL min^{-1} . Sample peaks were quantified at 201 nm and confirmed by comparing UV spectrum scans with spectrum scans of standards. Given that TCE is prone to volatilization, samples were collected in HPLC vials containing acetonitrile, completely filled (no headspace), and analyzed immediately.

MnO_4^- was measured with a HACH Spectrophotometer DR2800 (HACH Company, Loveland, CO) at a wavelength of 525 nm. Samples were diluted with water in 20-mL vials and filtered with 0.45 μm glass wool membrane prior to analysis to avoid any colloidal MnO_2 interference.

Changes in solution ^{14}C was determined by liquid scintillation counting (LSC) using a Packard 1900TR liquid scintillation counter (Packard instrument Co., Downers Grove, IL). Samples (8 mL) were added into a scintillation vial containing 15 mL Ultima GoldTM scintillation cocktail (Packard, Meriden, CT), unless stated otherwise, and mixed on a vortex mixer prior to analysis.

2D-Tank packing procedure

The 2D tank was hand packed with a rigorous set of steps and procedures to ensure uniformity between experiments. This involved using the same soil weights and template tools to produce a low permeable zone surrounded by a transmissive zone. In

brief, the steps used to pack the 2D tank were as follows: (1) the tank was divided into 7 layers before placing the transmissive sand into the tank; (2) after adding each layer of soil, we dry-packed the tank by gently packing with a specifically designed rubber hammer and shaking the tank horizontally at each packing level, (3) when the tank was packed to the height of the LPZ base, we marked the position of LPZ and inserted a plastic casing that fit closely inside the tank: (4) LPZ soils were then added to the casing using a funnel; (5) we removed the plastic casing once the LPZ and surrounding transmissive soil was packed (6) transmissive soil was pack above the LPZ and the top of the tank was reassembled.

Testing the ability of permanganate, with and without chemical amendments, to oxidize non-aqueous phase TCE under batch conditions

For the first set of batch experiments where TCE was placed in sand in a batch reactor, we tested 5 different solution treatments. These included: (1) control (no MnO_4^-); (2) MnO_4^- ; (3) MnO_4^- + PTPP; (4) MnO_4^- + SHMP; (5) MnO_4^- + TKPP. The concentrations of chemical additives used were the same as those used in the transport experiments (Table SM-2). Each group was also subcategorized into two MnO_4^- concentrations (i.e., 8000, and 16000 mg L^{-1}).

Sacrificial sampling occurred at, 2, 6, 9, and 14 d. Temporal changes in TCE and MnO_4^- concentration were monitored as described earlier. We determined the mass of TCE remaining in the experimental units by analyzing: (1) the solution above the transmissive sand, and (2) acetonitrile extracts of the transmissive sand. To quench samples treated with 16000 $\text{mg MnO}_4^- \text{ L}^{-1}$, we used 0.1 mL of 12.5% (v/v) hydrazine hydrate per 1.0 mL of sample. Likewise, we used 0.1 mL of 6.25% (v/v) hydrazine hydrate to quench samples treated with 8000 $\text{mg MnO}_4^- \text{ L}^{-1}$. To analyze the top solution, 0.5 mL of sample was withdrawn, quenched in a centrifuge tube containing 0.75 of

acetonitrile, and then centrifuged at 14000 rpm for 5 min. Supernatant was then transferred to an HPLC vial and immediately analyzed. TCE left in the sand was extracted with 20 mL of acetonitrile. The vessels were shaken on a reciprocal shaker for 15 min and 0.5 mL of extract was withdrawn, quenched, and centrifuged. Supernatant was then diluted with acetonitrile and analyzed.

Procedures used to extract and analyze LPZs cylinders

To differentiate the ^{14}C activity left in each experimental unit, the top solution (Portion 1) and LPZ cylinder, sand and entrained solution (Portion 2) were extracted separately using two different experimental units (Samples A and B).

For Sample A, 10 mL of the top solution (Portion 1) was transferred to a 40-mL glass tube containing 2 mL of 2.67 N HNO_3 and purged with N_2 gas for 10 min. This released TCE, CO_2 or volatile degradates from solution. After purging, 8 mL was then transferred to a scintillation vial containing 15 mL Ultima GoldTM scintillation cocktail and counted.

Portion 2 (sand, LPZ cylinder, and entrained solution) from Sample A received 2 mL of 2.67 N HNO_3 and was then shaken on a reciprocal shaker for 10 min to break apart the LPZ cylinder. The soil slurry was then purged with N_2 gas for 10 min. After purging, 4 mL of solution was transferred to a scintillation vial containing 15 mL Ultima GoldTM scintillation cocktail and counted.

For Sample B, 10 mL of the top solution (Portion 1) was transferred to a 40-mL glass vial containing 2.0 mL of 2.67 N HNO_3 and mixed with 10 mL of ethyl acetate. Then, 5 mL of the ethyl acetate were transferred to a vial containing 15 mL of Ultima GoldTM scintillation cocktail and counted. Portion 2 was treated with 2.0 mL of 2.67 N HNO_3 and 8 mL of ethyl acetate and shaken on a reciprocal shaker for 10 min. Eight mL of slurry solution were then transferred to a Teflon tube and centrifuged for 5000 rpm for 10 min. Two mL of the ethyl acetate were then transferred to a vial containing 15 mL of Ultima

GoldTM scintillation cocktail and counted. ¹⁴C-activity (i.e., dpms) determined in all samples were back calculated to original volumes. Activities in Portions 1 and 2 were added together to get ¹⁴C-activity of experimental unit for samples A and B.

The recovery of ¹⁴C-TCE in dpms was then calculated as:

$$^{14}\text{C-TCE} = ^{14}\text{C-activity of Sample B} - ^{14}\text{C-activity of Sample A} \quad [1]$$

Results and discussion

A parallel experiment to results presented in Sec. 3.2.1 tracked changes in solution pH for the various flooding treatments used in the transport and batch experiments. Results showed that the phosphorous containing compounds (SHMP, TKPP, PTPP) increased the pH above the water matrix (pH = 5.41) but when mixed with MnO_4^- , the pH of all treatments were between 6.30 and 6.86, with the exception of TKPP, which had a pH of 9.65 (Table SM-3). As expected, once the treatment solutions were mixed with TCE, the pH dropped as oxidation of TCE occurred and protons were generated. Depending on the treatment, the pH either bottomed out and then increased, or remained low. SHMP and PTPP were two chemical amendments that kept the pH low and close to that observed with MnO_4^- alone. By contrast, adding xanthan or TKPP caused the pH to decrease but then increase to near neutral pH values with later samplings (Table SM-3). Because significant differences were noted in the temporal pH values of the flooding solutions, we determined if this correlated with the mass of MnO_2 precipitation formed. When we filtered the flooding solutions through a 25 μm filter (Whatman, Piscataway, NJ), we observed that MnO_4^- and $\text{MnO}_4^- + \text{xanthan}$, had the highest mass of filterable MnO_2 , followed by $\text{PTPP} > \text{TKPP} > \text{SHMP}$.

Tables

Table SM-1

Chemical properties

Chemical	Molecular Formula	Description	M.W. (g mol ⁻¹)	Density (g cm ⁻³)	Viscosity (cP)	Solubility (mg L ⁻¹)	Manufacturer
Trichloroethene (TCE)	C ₂ HCl ₃	Contaminant	131.39	1.48 ⁽¹⁾	0.58 ⁽²⁾	1101 ⁽¹⁾	Sigma Aldrich (ACS grade)
Xanthan gum	(C ₃₅ H ₄₉ O ₂₉) _n (monomer)	Soluble polymer	(933) _n (monomer)	0.998 ⁽³⁾	Variable	>5000 ⁽³⁾	Sigma Aldrich
Sodium Permanganate	NaMnO ₄	Oxidizing agent	141.93	1.972	-	Liquid	Aldrich Chemistry
Potassium Permanganate	KMnO ₄	Oxidizing agent	158.03	2.70	~1.0	~60000	Sigma Aldrich (ACS grade)
Pentyltriphenylphosphonium Bromide (PTPP)	C ₂₃ H ₂₆ P·Br	Phase transfer catalyst	413.35 ⁽⁴⁾	-	-	2.4 x 10 ⁻⁴ (⁴)	Aldrich Chemistry
Sodium Hexametaphosphate (SHMP)	(NaPO ₃) ₆	Dispersing Agent	611.77	2.484	-	Soluble	Sigma Aldrich
Tetrapotassium Pyrophosphate (TKPP)	K ₄ P ₂ O ₇	Dispersing Agent	330.34	-	-	Highly soluble	Carus Corporation
Oil-red-O	C ₂₆ H ₂₄ N ₄ O	Visual aid	408	-	-	Slightly soluble	Sigma Aldrich

¹[33]; ²[51]; ³[6]; and ⁴[32] (see main manuscript for references)

Table SM-2

Solutions, concentrations, and pore volumes used in transport experiments

Exp	Initial Flood Concentrations (mg L ⁻¹)					Secondary Flood	Total PV
	MnO ₄ ⁻	Xanthan	SHMP	TKPP	PTPP	CaCl ₂ (441 mg L ⁻¹) PV	
A	9931	-	-	-	-	15.5	16.00
B	9931	500	-	-	-	15.5	16.00
C	9931	-	1000	-	-	15.5	16.00
D	9931	-	-	-	51.16	15.5	16.00
E	9931	-	-	1000	-	15.5	16.00
F	9931	500	1000	-	-	15.5	16.00

Table SM-3

Temporal changes in pH of flooding solutions used to treat non-aqueous phase TCE under batch conditions.

Treatments ¹	Initial pH		pH following treatment of							Filterable Precipitates ³ at T = 336 h (mg)
	- MnO ₄ ⁻	+ MnO ₄ ⁻	TCE (non-aqueous phase) ²							
			4 h	24 h	48 h	72 h	168 h	264 h	336 h	
A. MnO ₄ ⁻	5.41	6.65	2.32	2.22	2.22	2.23	2.33	2.43	2.43	97.7
B. MnO ₄ ⁻ + Xanthan	5.77	6.30	2.47	5.03	5.38	5.92	6.70	7.01	7.28	123.9
C. MnO ₄ ⁻ + SHMP	7.42	6.56	2.63	2.31	2.35	2.39	2.42	2.46	2.41	61.5
D. MnO ₄ + TKPP	10.07	9.65	6.93	3.80	4.42	5.16	5.70	5.82	5.96	61.7
E. MnO ₄ + PTPP	7.69	6.86	2.42	2.20	2.15	2.12	2.14	2.24	2.21	77.6
F. MnO ₄ ⁻ + Xanthan + SHMP	7.14	6.47	3.27	3.09	4.59	4.89	6.25	6.51	6.74	117.9

¹¹Concentrations of chemical treatments used are listed in Table SM-2; pH of H₂O = 5.41

^{2,3}Samples were measured in quadruplicate

Figures

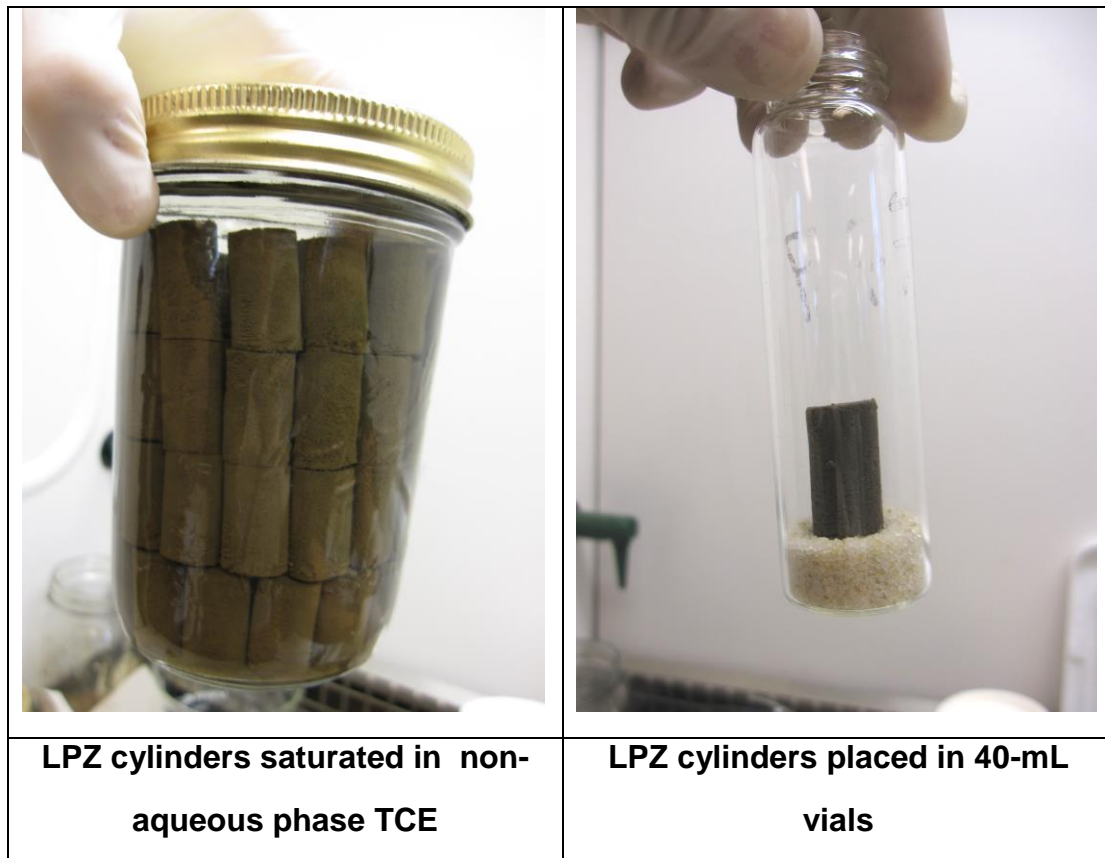


Figure SM-1. Photographs of low-permeable zone (LPZ) cylinders used in batch experiments.

25
 26
 27
 28
 29
 30
 31
 32
 33
 34
 35
 36
 37
 38
 39
 40
 41
 42
 43
 44
 45
 46
 47
 48
 49
 50

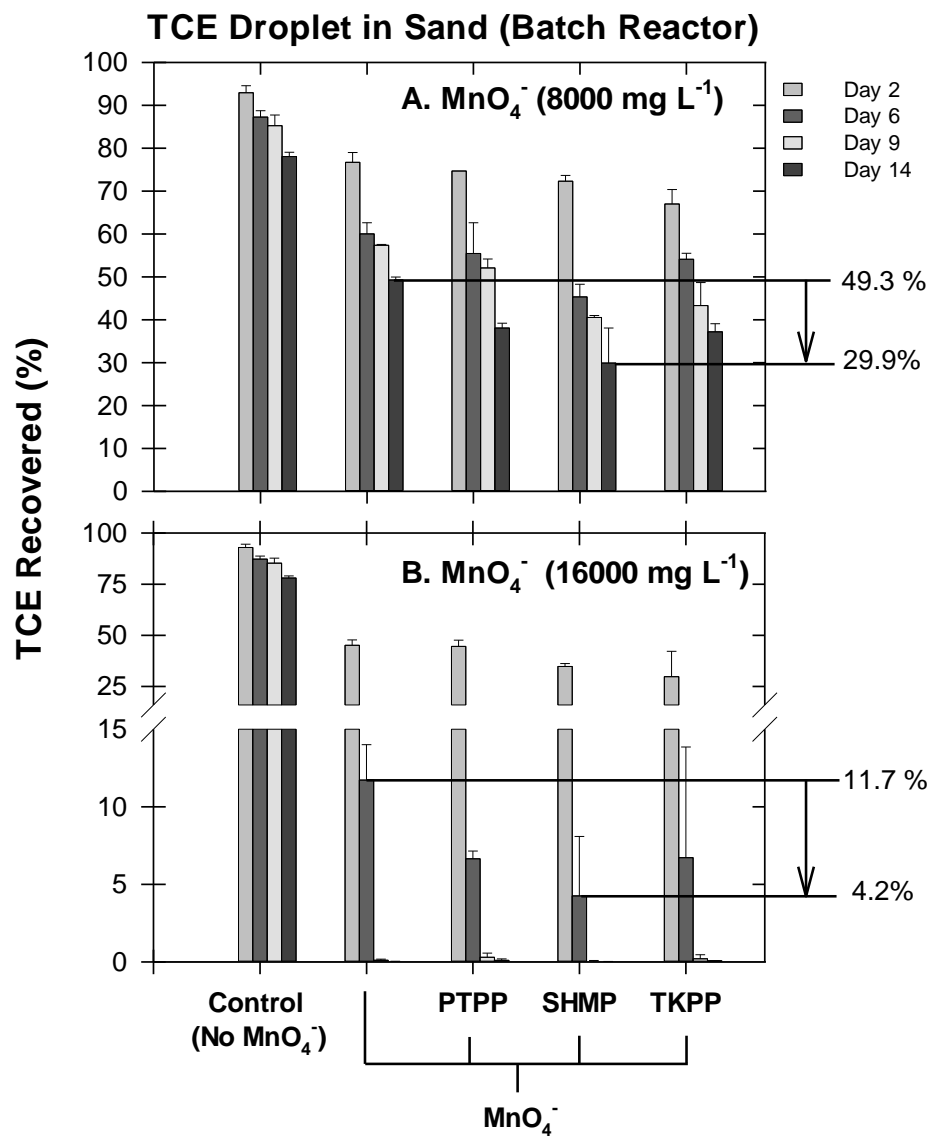


Figure SM-2. Effect of MnO_4^- , with and without chemical amendments, on non-aqueous phase TCE recovery. TCE was placed in transmissive sands in a batch reactor.

51
52
53
54
55
56
57
58
59
60
61
62
63
64
65
66
67
68
69
70
71
72
73
74
75
76

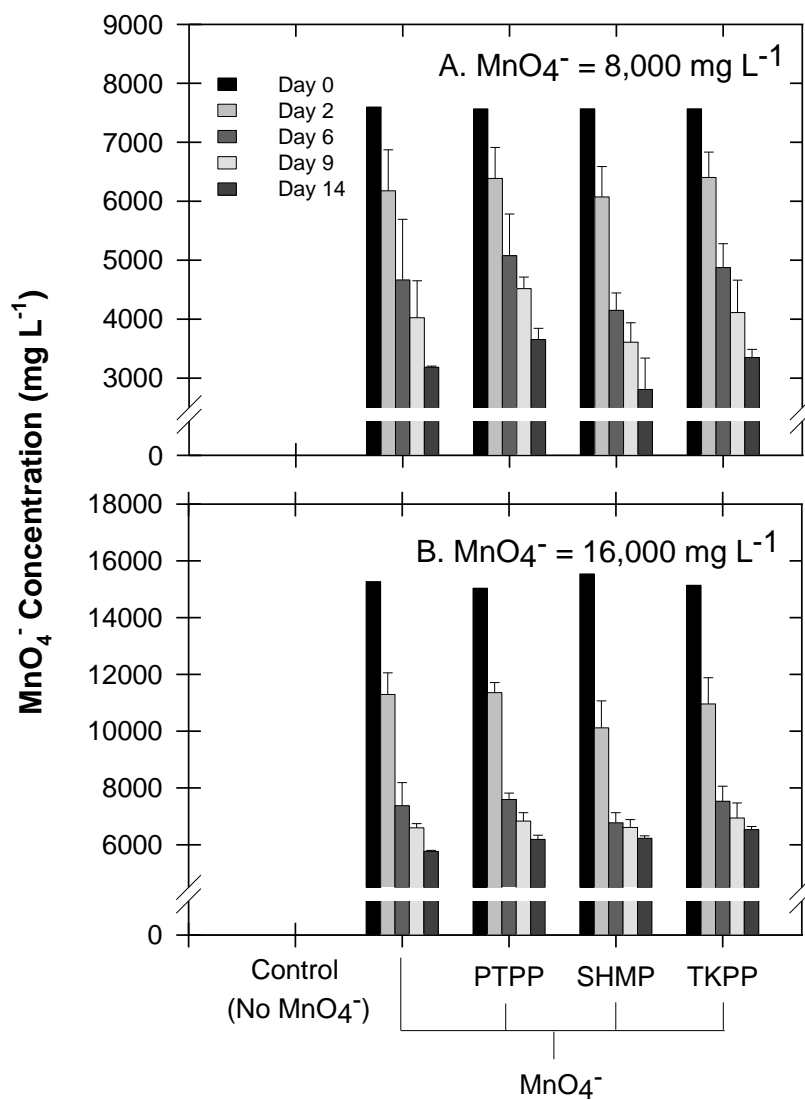


Figure SM-3. Temporal changes in MnO_4^- concentrations following treatment of non-aqueous phase TCE with various MnO_4^- flooding solutions. TCE was placed in transmissive sands in a batch reactor.

77
78
79
80
81
82
83
84
85
86
87
88
89
90
91
92
93
94
95
96
97
98
99
100
101
102

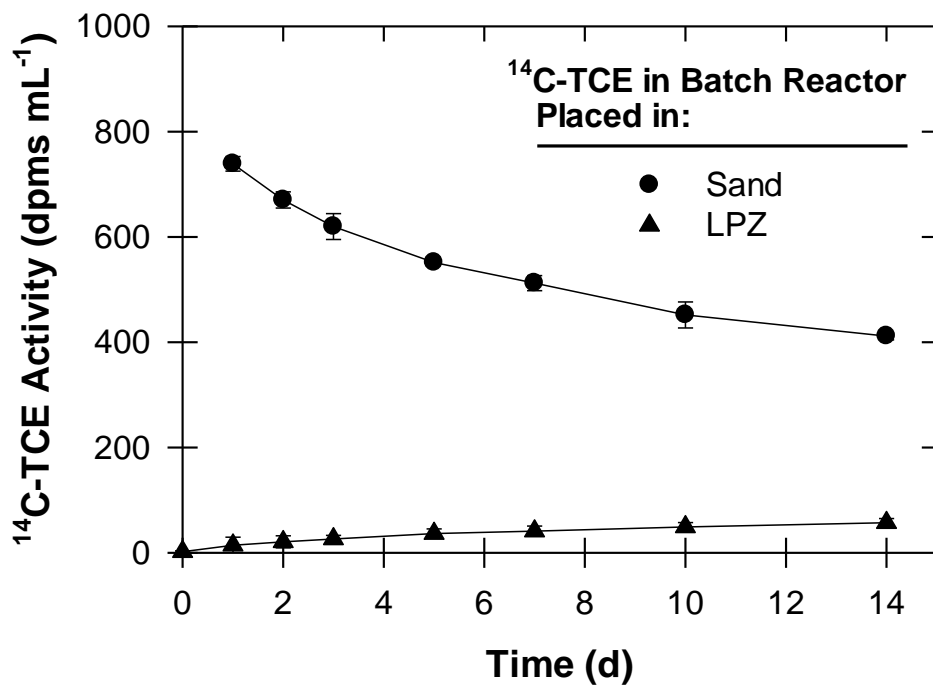


Figure SM-4. Release of ¹⁴C-TCE into solution from non-aqueous TCE that was placed in batch reactor containing sand versus a LPZ cylinder.

103
104
105
106
107
108
109
110
111
112
113
114
115
116
117
118
119
120
121
122
123
124
125
126
127
128

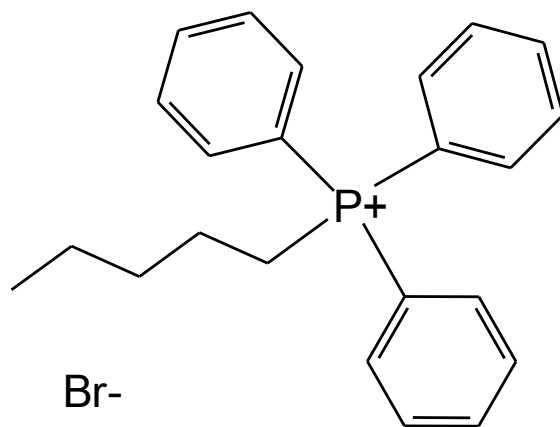


Figure SM-5. Pentyltriphenylphosphonium Bromide (PTPP) molecular structure.

129
130
131
132
133
134
135
136
137
138
139
140
141
142
143
144
145
146
147
148
149
150
151
152
153
154

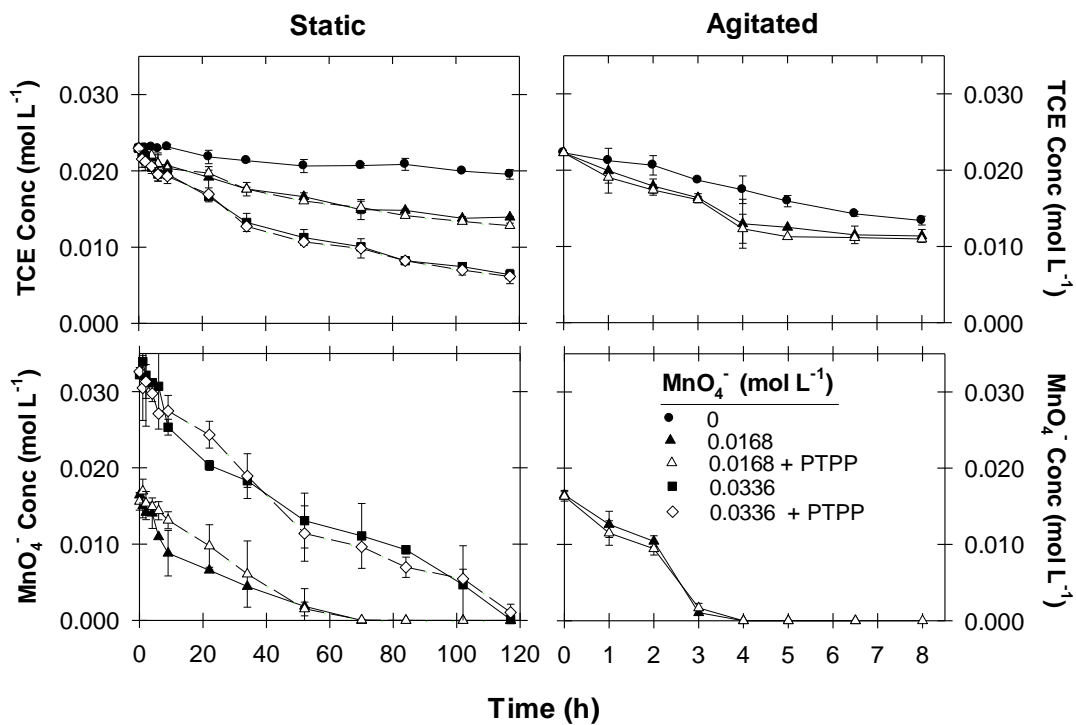


Figure SM-6. Tests of the phase-transfer catalyst, PTPP, on improving TCE removal by MnO₄⁻ under static and agitated conditions.